JOURNAL OF THE KOREAN ASTRONOMICAL SOCIETY
33: 47 ~ 55, 2000

NONPOTENTIAL PARAMETERS OF SOLAR ACTIVE REGION AR 5747

Y.-J. MOON[1], H. S. YUN[2], GWANGSON CHOE[3], Y. D. PARK[1], AND D. L. MICKEY[4]
[1]Bohyunsan Optical Astronomical Observatory, Korea Astronomy Observatory, Kyungpook 770-820
[2]Astronomy Program, SEES, Seoul National University, Seoul 151-742
[3]Princeton Plasma Physics Laboratory, Princeton, NJ 08543-0451, USA
[4]Institute for Astronomy, University of Hawaii, 2680 Woodlawn Drive, Honolulu, HI 96822-1839, USA
E-mail: yjmoon@boao.re.kr
(Received Apr. 24, 2000; Accepted May 28, 2000)

ABSTRACT

Nonpotential characteristics of magnetic fields in AR 5747 are examined using Mees Solar Observatory magnetograms taken on Oct. 20, 1989 to Oct. 22, 1989. The active region showed such violent flaring activities during the observational span that strong X-ray flares took place including a 2B/X3 flare. The magnetogram data were obtained by the Haleakala Stokes Polarimeter which provides simultaneous Stokes profiles of the Fe I doublet 6301.5 and 6302.5. A nonlinear least square method was adopted to derive the magnetic field vectors from the observed Stokes profiles and a multi-step ambiguity solution method was employed to resolve the 180° ambiguity. ¿From the ambiguity-resolved vector magnetograms, we have derived a set of physical quantities characterizing the field configuration, which are magnetic flux, vertical current density, magnetic shear angle, angular shear, magnetic free energy density, a measure of magnetic field discontinuity MAD and linear force-free coefficient. Our results show that (1) magnetic nonpotentiality is concentrated near the inversion line in the flaring sites, (2) all the physical parameters decreased with time, which may imply that the active region was in a relaxation stage of its evolution, (3) 2-D MAD has similar patterns with other nonpotential parameters, demonstrating that it can be utilized as an useful parameter of flare producing active region, and (4) the linear force-free coefficient could be a evolutionary indicator with a merit as a global nonpotential parameter.

Key words : Sun : magnetic fields – Sun : sunspot – Sun : flare

I. INTRODUCTION

It is generally believed that magnetic fields play a central role in solar eruptive phenomena such as flares and coronal mass ejections. The energy released through solar eruptive processes is considered to be stored in nonpotential magnetic fields. The magnetic energy is supplied to the corona either by plasma flows moving around magnetic fields in the inertia-dominant photosphere or by magnetic flux emerging from below the photosphere. Since measurements of magnetic fields at the coronal altitude are not available, magnetograms taken at the photospheric level have been widely used for studies of magnetic nonpotentiality in flare-producing active regions and are also used through extrapolation to compute coronal magnetic fields.

Several attempts have been made to identify the relationship between time variation of nonpotentiality parameters and development of solar flares (Hagyard et al. 1984, Hagyard et al. 1990, Wang et al. 1996, Wang 1997). Moon et al. (2000) reviewed previous studies on magnetic nonpotentiality indicators and discussed the problems involved in them. Specifically, they studied the evolution of nonpotentiality parameters in the course of an X-class flare of AR 6919 using MSO (Mees Solar Observatory) magnetograms. They showed that the magnetic shear obtained from the vector magnetograms increased just before the flare and then decreased after it, at least near the δ spot region. Moon et al. (1999) proposed a measure of magnetic field discontinuity, MAD, defined as Maximum Angular Difference between two adjacent field vectors, as a flare activity indicator. They applied this concept to three magnetograms of AR 6919 and found that the high MAD regions well match the soft X-ray bright points observed by Yohkoh. It was also found that the MAD values increased just before an X-class flare and then decreased after it. This paper constitutes one of the series of studies on evolution of magnetic nonpotentiality associated with major X-ray flares, which are performed using MSO vector magnetograms.

On the other hand, the problem whether magnetic fields at the photospheric level are force-free or not is of significance for understanding the evolution of coronal magnetic field structures (Metcalf et al. 1995). Pevtsov et al. (1997) analyzed 655 photospheric magnetograms of 140 active regions to examine the spatial variation of the force-free coefficient. In their results, some of the active regions show good correlation between B_z and J_z, but others do not. It is very natural that the force-free coefficient varies depending on active region in question even when the coefficient is more or less constant over the active region. If we can draw a force-free coefficient from the magnetic fields of an active

region, it could be a good nonpotential parameter.

The purpose of this paper is to examine the magnetic nonpotentiality of AR 5747 associated with solar flares. For this study, we have used a set of high quality magnetograms spanning three days obtained from full Stokes polarization profiles of MSO and calibrated them by the non-linear least square method. Thus our data should be able to yield a more reasonable estimate of various nonpotentiality parameters. Since we have only one magnetogram in a day, we can not expect such an abrupt change of magnetic nonpotentiality as Wang (1992) found. In our study, emphasis is given to the long-term evolution of magnetic nonpotentiality with the progress of several major X-ray flares which occurred in AR 5747. In Section II, an account is given of the magnetic nonpotentiality parameters that we have considered in this study. In Section III, a description is given of the observation and analysis of the vector magnetograms. Computation of nonpotentiality parameters and their characteristics are presented in Section IV. Finally, a summary and conclusion are given in Section V.

II. MAGNETIC NONPOTENTIAL PARAMETERS

(a) Electric Current Density

It is well accepted that electric currents play an important role in the process of energy buildup and relaxation of solar active regions. Since the observation of vector magnetic fields is available only in the photosphere, the vertical current at the photosphere is widely used in studies of solar active regions.

According to Ampere's law, the vertical current density is given by

$$J_z = \frac{c}{4\pi}\left(\frac{\partial B_y}{\partial x} - \frac{\partial B_x}{\partial y}\right). \tag{1}$$

In this work, we use the four-point differentiation method to compute vertical current density.

(b) Magnetic Angular Shear

Hagyard et al. (1984) defined the magnetic angular shear (or magnetic shear) as the angular difference between the observed transverse field and the azimuth of the transverse component of the potential field which is computed employing the observed longitudinal field as a boundary condition. That is, the magnetic angular shear θ_a is given by

$$\theta_a = \theta_o - \theta_p\,, \tag{2}$$

in which $\theta_o = \arctan(B_y/B_x)$ is the azimuth of observed transverse field and $\theta_p = \arctan(B_{px}/B_{py})$ is that of the corresponding potential field component. Noting that flares are associated with magnetic shear of strong transverse fields, Wang (1992) proposed a transverse weighted mean angular shear given by

$$\overline{\theta}_a = \frac{\sum B_t\theta_a}{\sum B_t}\,, \tag{3}$$

in which B_t is the transverse field strength and the sum is taken over all the pixels in the considered region. In this work we use horizontal field strength in the heliographic coordinate instead of transverse field strength.

(c) Magnetic Shear Angle

Lü et al. (1993) suggested a new nonpotentiality indicator, the angle between the observed magnetic field vector and the corresponding potential magnetic field vector. By definition, the shear angle θ_s can be expressed as

$$\theta_s = \arccos\left(\frac{\mathbf{B_o}\cdot\mathbf{B_p}}{|\mathbf{B_o}||\mathbf{B_p}|}\right), \tag{4}$$

where $\mathbf{B_o}$ and $\mathbf{B_p}$ are the observed and potential magnetic field vectors, respectively. In this equation, B_{pz} is identical with B_{oz} as explained earlier. In our study, we proceed a step further and consider a field strength weighted mean shear angle defined by

$$\overline{\theta}_s = \frac{\sum |\mathbf{B}|\theta_s}{\sum |\mathbf{B}|}\,, \tag{5}$$

where $|\mathbf{B}|$ is the field strength and the sum is taken over all the pixels in the considered region.

(d) Magnetic Free Energy Density

The density of magnetic free energy is given by

$$\rho_f = \frac{(\mathbf{B_o}-\mathbf{B_p})^2}{8\pi} = \frac{\mathbf{B_s}^2}{8\pi}\,, \tag{6}$$

where $\mathbf{B_s}$ is the nonpotential part of the magnetic field, which was defined as the source field by Hagyard, Low, and Tandberg-Hanssen (1981). It can also be expressed as (Wang et al. 1996)

$$\rho_f = \frac{(|\mathbf{B_o}| - |\mathbf{B_p}|)^2}{8\pi} + \frac{|\mathbf{B_o}||\mathbf{B_p}|}{2\pi}\sin^2(\theta_s/2)\,, \tag{7}$$

where $|\mathbf{B_o}|$ and $|\mathbf{B_o}|$ are magnitudes of the observed field and the computed potential field, respectively. The tensor virial theorem can be utilized to estimate the total magnetic free energy of a solar active region (e.g., Metcalf et al. 1995). However, as McClymont et al. (1997) pointed out (for details, see Appendix A of their paper), there are several controversial problems in estimating the magnetic free energy of a real active region with this method. In this study, we examine an observable quantity, the sum of magnetic free energy density over a field of view. This quantity is expected to indicate the degree of nonpotentiality at least near the photosphere.

(e) MAD : A Measure of Magnetic Field Discontinuity

Magnetic topology is widely used for understanding the role of magnetic fields while flaring activity (Demoulin et al. 1993, Demoulin et al. 1996). A separator is known as a good candidate as a site of current sheet formation. In the vicinity of a separator, the magnetic field generally changes its direction and magnitude quite abruptly. When we are given a set of discrete data of magnetic field vectors, the local maxima of the angular difference between two adjacent field vectors can be employed to locate a separator and further a current sheet.

On this basis, Moon et al. (1996, 1999) suggested the MAD as

$$\mathrm{MAD} = \max\left[\frac{180}{\pi}\arccos\left(\frac{\mathbf{B_o}\cdot\mathbf{B_i}}{|\mathbf{B_o}||\mathbf{B_i}|}\right)\ (i=1\sim 6)\right], \tag{8}$$

where $\mathbf{B_o}$ is the magnetic field vector at a given position (x,y,z) and $\mathbf{B_i}$ is one of the six adjacent field vectors in the 3-D grid . If two adjacent magnetic fields are antiparallel, the MAD becomes 180°. In a similar way one can define the 2-D MAD in an observing x-y plane. In this study, we consider a field strength weighted 2-D MAD to reduce the uncertainty induced by polarization measurement errors of weak field regions.

(f) Linear Force-Free Coefficient

If magnetic fields in an active region are approximately linear force-free, the linear force-free coefficient α is given by

$$\alpha = \frac{J_z}{B_z} \tag{9}$$

in rationalized electromagnetic units. In practice, the linear force-free coefficient can be drawn from the linear regression between J_z and B_z. While the nonpotential parameters above represent nonpotential characteristics of a localized region, the linear force-free coefficient should be regarded as a nonpotential parameter which characterizes the global structure of magnetic fields in a given field of view.

III. OBSERVATION AND ANALYSIS

For the present work, we have selected a set of MSO magnetograms of AR 5747 taken on Oct. 20–22, 1989. The magnetogram data were obtained by the Haleakala Stokes polarimeter (Mickey, 1985) which provides simultaneous Stokes I,Q,U,V profiles of the Fe I 6301.5, 6302.5 Å doublet. The observations were made by a rectangular raster scan with a pixel spacing of 5.6″ (low resolution scan) and a dispersion of 25 mÅ/pixel. Most of the analyzing procedure is well described in Canfield et al. (1993). To derive the magnetic field vectors from Stokes profiles, we have used a nonlinear least square fitting method (Skumanich and Lites, 1987) for fields stronger than 100 G and an integral method (Ronan, Mickey and Orral, 1987) for weaker fields. In that fitting, the Faraday rotation effect, which is one of the error sources for strong fields, is properly taken into account. The noise level in the original magnetogram is about 70 G for transverse fields and 10 G for longitudinal fields. The basic observational parameters of the magnetograms used in this study are presented in Table 1.

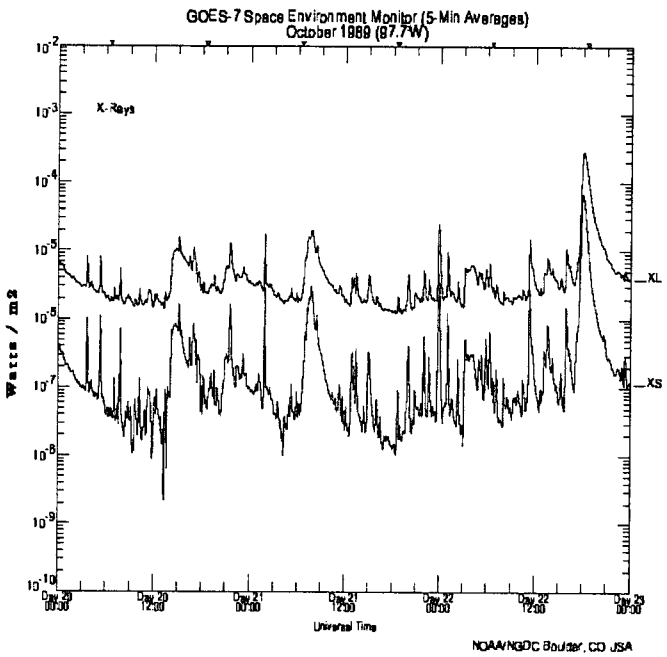

Fig. 1.— GOES 5 minute averages of soft X-ray fluxes from Oct. 20 to 22, 1989. Here XL represents long X-ray fluxes (1-8Å) and XS, short X-ray fluxes (0.5-4Å). In the y-axis, $10^{-5}Watt/m^2$ correspond to a peak flux of M1 class flare.

To resolve the 180° ambiguity, we have adopted a multi-step ambiguity solution method by Canfield et al. (1993) (for details, see the Appendix of their paper). In the 3rd and 4th steps of their method, they have chosen the orientation of the transverse field that minimizes the angle between neighboring field vectors and the field divergence $|\nabla\cdot\mathbf{B}|$.

IV. MAGNETIC NONPOTENTIALITY

In the active region AR 5747, a number of flares took place including a 2B/X3 flare. Figure 1 shows GOES soft X-ray fluxes from Oct. 20 to Oct. 22, 1989. As seen in the figure, there are seven major flares stronger than M1 class, whose basic features during the observing period are summarized in Table 2.

Figure 2 shows the ambiguity resolved vector magnetograms obtained on Oct. 20 to Oct. 22, 1989. The three magnetograms have the same field of view. As

Table 1. Basic observational parameters of AR 5747.

Data	Date	Time	Scan	Data Points	Coord.
AR5747 a)	20 Oct., 1989	17:41-18:50	5.656″	30×30	S26W07
AR5747 b)	21 Oct., 1989	19:20-20:16	5.656″	30×30	S26W22
AR5747 c)	22 Oct., 1989	18:27-19:41	5.656″	30×40	S26W33

Table 2. Basic information of the major X-ray flares observed in AR 5747 (Solar Geophysical Data).

ID	Date	Start(UT)	End	Max.	Coord.	Optical Class	X-ray Class
F1	20/10/89	21:30	22:03	21:34	S26W11	1N	M1.4
F2	21/10/89	01:53	02:06	01:55	S28W09	1N	M2.4
F3	21/10/89	06:40	06:49	06:43	S27W16	1N	M1.9
F4	21/10/89	23:54	24:00	23:56	S28W22		M3.1
F5	22/10/89	11:15	12:30	11:21	S27W26	SN	M1.5
F6	22/10/89	15:54	16:47	15:58	S28W28	SN	M1.3
F7	22/10/89	17:08	21:08	17:57	S27W31	2B	X2.9

seen from the figures, strong sheared transverse fields are concentrated near the neutral line and they form a global clockwise winding pattern. The vertical current density is presented in Figure 3, where its kernels persisted, with little change of configuration, over the whole observing span. Wang, Xu, and Zhang (1994) and Leka et al. (1993) have discussed the important characteristics of these vector magnetic fields and vertical current densities. We tabulate the time variation of magnetic fluxes and total vertical currents of positive and negative signs in Table 3. The differences between the absolute values of the positive and negative quantities are within a few percent. As seen from the table, the magnetic fluxes and total vertical currents of both signs decreased with time. It is observed that several small δ sunspots (A1, A2 and A3 in Fig. 2a) disappeared in Figure 2b, which suggests that flaring events between Oct. 20 and 21 should be associated with flux cancellation. It is to be noted that there were no remarkable flux emergence during the observing period.

Figure 4 shows the angular shear multiplied by transverse field strength and Figure 5 shows the shear angle multiplied by total field strength. As seen from the figures, strong magnetic shear is concentrated near the inversion line, where H_β emission patches were observed (see Fig. 2 of Wang, Xu, and Zhang 1994). The time variation of two weighted mean shear angles is given in Table 4. The values of two shear angles monotonically decreased with time. The magnetic free energy density is shown in Figure 6. Its evolutionary trend is quite similar to that of shear angles. The 2-D MAD multiplied by total field strength (Figure 7) also has a similar evolutionary pattern to that of the other nonpotentiality parameters above. We summarize the variations of mean free energy density, planar sum of free energy density, and sum of MAD multiplied by field strength in Table 4, in which the values obtained with the potential field method for the 180° ambiguity resolution are also given in parentheses for comparison.

Now we turn to the question whether our active region field is approximately linearly force-free. Moon (1999) already showed that the magnetic fields of AR 5747 are approximately force-free from the calculation of integrated magnetic pressure forces. In Figure 2, the transverse field vectors show a common curling pattern for each magnetic polarity, which allows us to expect that values of the force-free coefficient do not diverge much. To investigate the linearity, we have plotted for each data set B_z vs. J_z and a plausible regression line obtained by eye fitting in Figure 8. The figures show that there exists an approximate linear relationship between B_z and J_z for three vector magnetograms. We have already observed in Figure 2 and Figure 3 that the distribution of vertical electric current density well matches that of magnetic fluxes with the corresponding polarity. In Table 4, we have tabulated linear force-free coefficients obtained by linear regression in Figure 8. As seen from the table, the absolute value of force-free coefficients decreased with time, as other nonpotentiality parameters did. This suggests that the linear force-free coefficient could be as a good nonpotential evolutionary indicator as long as the linear force-free approximation is more or less valid. Furthermore, the linear force-free coefficient has a merit as a global parameter.

¿From the above results, we may infer that the flares that occurred in our observation are just bursty parts of energy release in a long-term relaxation of the stressed magnetic field. In a self-organizing system, a transition toward a lower energy state proceeds very mildly in the beginning and for most of time until a sudden bursty event develops as in an avalanche. Why, then,

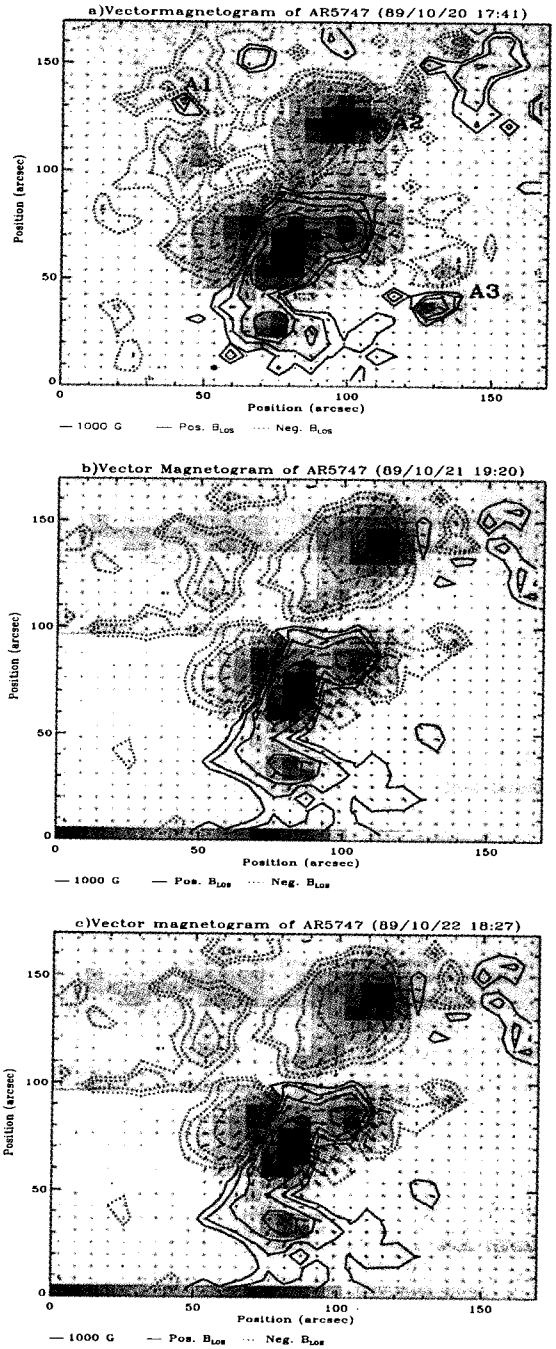

Fig. 2.— Three MSO vector magnetograms of AR 5747 superposed on white light images taken on Oct. 20–22, 1991. In all the figures, the solid lines stand for positive polarity and the dotted lines for negative polarity. The contour levels correspond to 100, 200, 400, 800 and 1600 G, respectively. The length of arrows represents the magnitude of the transverse field components.

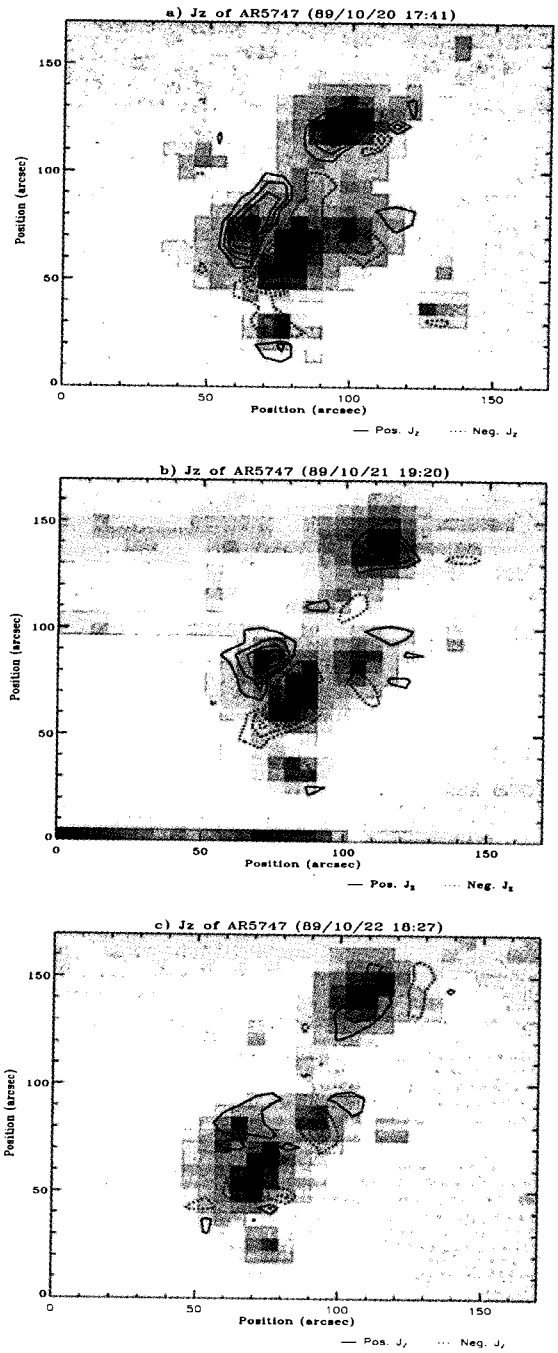

Fig. 3.— Contours of vertical current density in AR 5747. The contour levels correspond to 3, 6, 9, 12 and 15 mA/m^2, respectively. In all the panels, the solid lines stand for positive vertical current density and the dotted lines for negative current density.

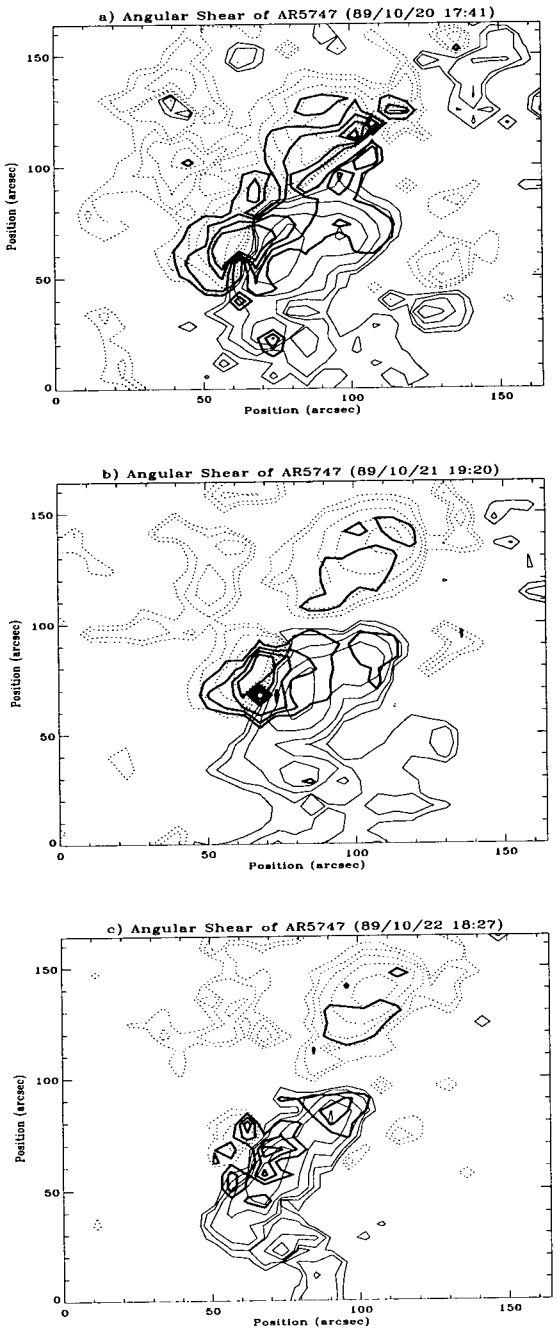

Fig. 4.— Contours of angular shear multiplied by transverse field strength drawn in thick solid lines are superposed on longitudinal magnetograms. The contour levels are 4.0×10^4, 7.0×10^4, 1.0×10^5 and 1.3×10^5 G deg, respectively. In all the panels, the solid lines stand for positive longitudinal polarity and the dotted lines for negative one. The contour levels in the magnetograms correspond to 100, 200, 400, 800 and 1600 G, respectively.

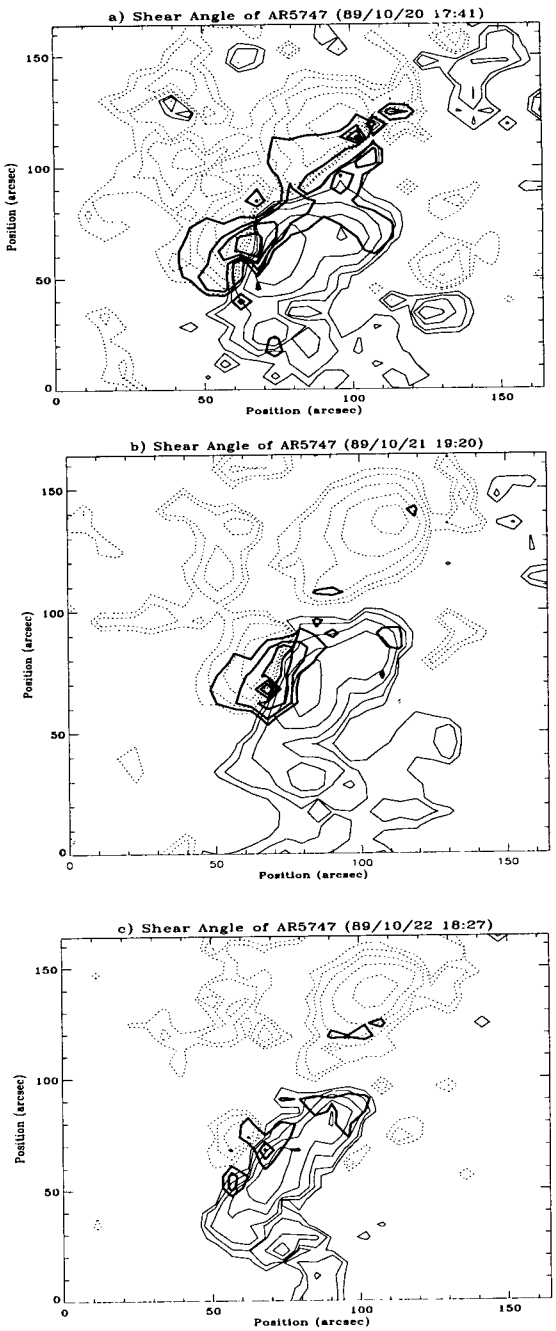

Fig. 5.— Contours of shear angle multiplied by field strength drawn in thick solid lines are superposed on longitudinal magnetograms. The contour levels are 4.0×10^4, 7.0×10^4, 1.0×10^5 and 1.3×10^5 G deg, respectively. The magnetograms are the same as in Fig. 4.

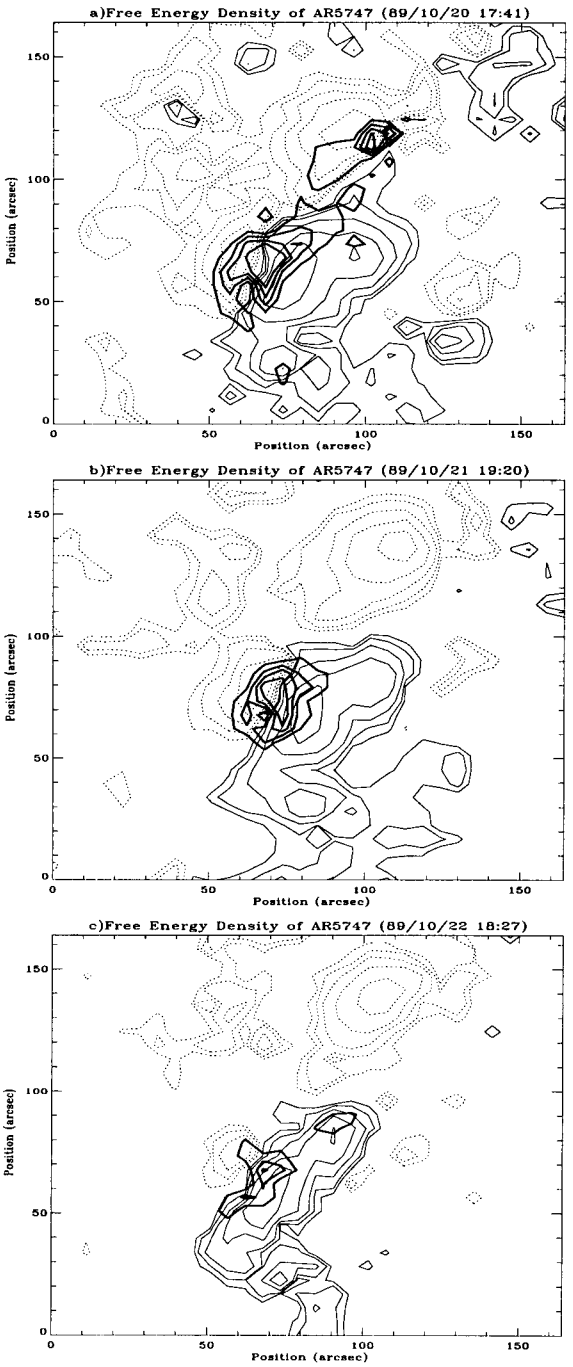

Fig. 6.— Contours of free energy density drawn in thick solid lines are superposed on magnetograms. The contour levels are 5.0×10^4, 1.0×10^5, 1.5×10^5, 2.0×10^5 and 2.5×10^5 erg/cm^3, respectively. The magnetograms are the same as in Fig. 4.

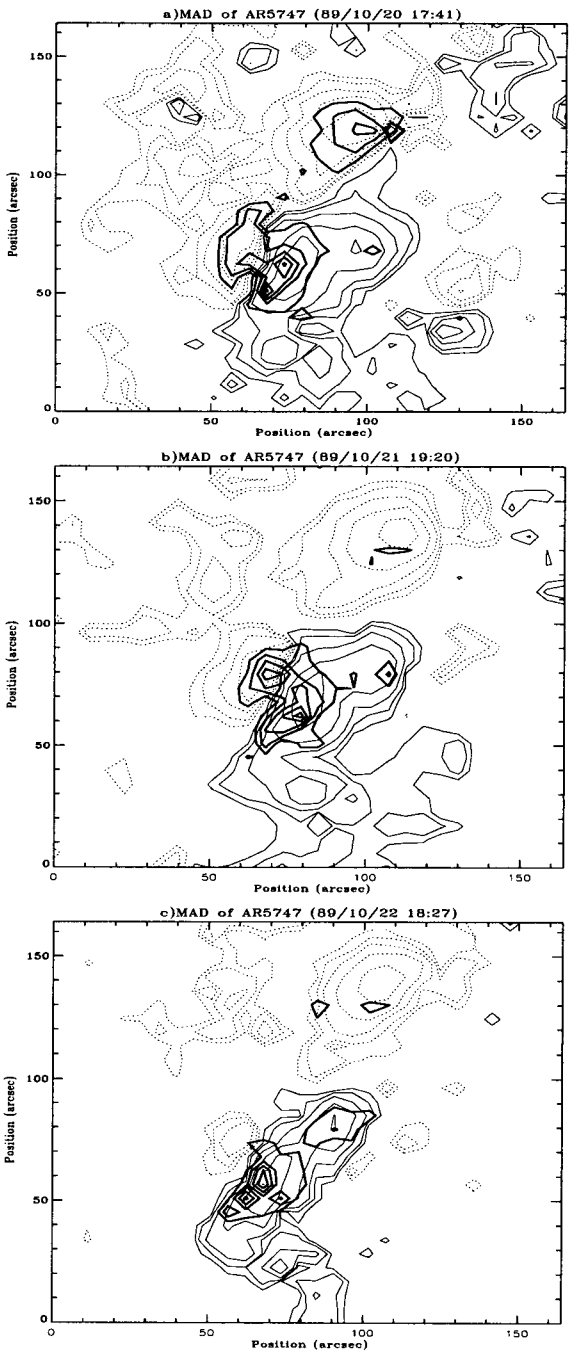

Fig. 7.— Contours of MAD multiplied by field strength drawn in thick solid lines are superposed on longitudinal magnetograms. The contour levels are 3.0×10^4, 5.0×10^4, 7.0×10^4, 9.0×10^4 and 1.1×10^5 G deg, respectively. The magnetograms are the same as in Fig. 4.

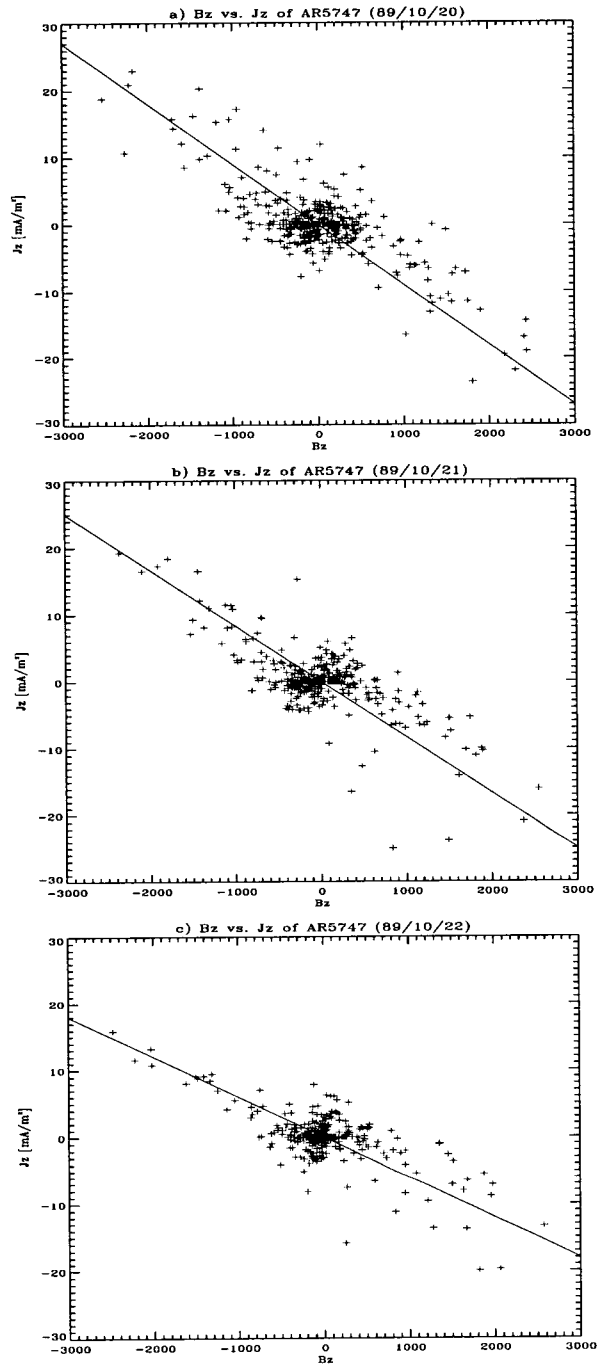

Fig. 8.— J_z vs. B_z from three vector magnetograms of AR 5747. Straight lines are the regression lines obtained from eye fitting.

did a series of flares occur, rather than one? Flares can surely take place in repetition if enough energy is supplied into the system between the flaring events to recover the free energy released by the preceding flaring event. However, this is not the case as far as the flares in our observation are concerned. No indication of energy input, regardless of flux emergence or increase of magnetic shear, was detected throughout our observing span. We thus speculate that the occurrence of a series of flares was possible due to the complex geometry of our active region magnetic field. A simple bipolar magnetic field would proceed to a lower energy state by one bursty event of reconnection. However, in a complex active region containing more than a pair of magnetic poles, the transition to the lowest energy state may possibly comprise several steps of macroscopic change in field topology. This speculation, of course, has to be examined by further studies involving many other observations and numerical experiments as well.

V. SUMMARY AND CONCLUSION

In this study, we have analyzed the MSO vector magnetograms of AR 5747 taken on October 20 to 22, 1989. A nonlinear least square method was adopted to derive the magnetic field vectors from the observed Stokes profiles and a multi-step ambiguity solution method was used to resolve the 180° ambiguity. ¿From the ambiguity-resolved vector magnetograms, we have derived a set of physical quantities which are magnetic flux, vertical current density, magnetic shear angle, angular shear, magnetic free energy density, a measure of magnetic field discontinuity, and linear force-free coefficient. In order to derive the force-free coefficient of the active region field, we have compared the longitudinal field B_z and the corresponding vertical current density J_z. Most important results from this work can be summarized as follows.

1) Magnetic nonpotentiality is concentrated near the inversion line, where flare brightenings are observed.

2) All the physical parameters that we have considered (vertical current density, mean shear angle, mean angular shear, sum of free energy density, sum of MAD, and linear force-free coefficient) decreased with time, which may indicate that the active region was in a relaxation period. It is also noted that three magne-

Table 3. Magnetic fluxes and total vertical currents in AR 5747 for three different times in the observing period. Here σ_J denotes the standard deviation of the vertical current distribution.

Data	F(+)[Mx]	F(-)	$\sum J_z^+$[A]	$\sum J_z^-$	σ_J
a)	1.6E22	1.5E22	6.7E4	6.6E4	1.4
b)	1.3E22	1.3E22	4.2E4	4.2E4	1.2
c)	0.9E22	0.9E22	3.9E4	4.0E4	1.2

Table 4. Field strength weighted mean magnetic shear angle $\bar{\theta}_s$, transverse field weighted angular shear $\bar{\theta}_a$, mean free energy density $\bar{\rho}_f$, planar sum of magnetic free energy density $\sum \rho_f$, $\sum$(MAD × |B|), and linear force-free coefficients α for AR 5747 for three different times. The values in parentheses are obtained employing the potential field method.

Data	$\bar{\theta}_s$	$\bar{\theta}_a$	$\bar{\rho}_f$[erg/cm^3]	$\sum \rho_f$[erg/cm]	$\sum$(MAD × |B|)	α[m^{-1}]
a)	46.8(38.4)	71.8(56.1)	2.7(2.0)E4	1.4(1.0)E24	4.7E6	-1.1×10^{-7}
b)	41.3(36.3)	63.0(53.4)	2.1(1.6)E4	9.3(6.9)E23	3.5E6	-1.0×10^{-7}
c)	36.1(32.6)	55.7(48.3)	1.7(1.4)E4	5.1(4.3)E23	2.3E6	-7.2×10^{-8}

tograms used in this study does not have sufficient time resolution for identifying the relationship between individual flares and energy release process.

3) 2-D MAD has similar patterns with other nonpotential parameters, expecting that it can be utilized as a useful parameter of flare producing active region.

4) The linear force-free coefficient could be a nonpotential parameter with a merit as a global one as long as magnetic fields in an active region are approximately linear force-free.

5) The X-ray flares that occurred during the observing period could be related with flux cancellation. Flaring events might be considered as bursty parts in the long-term relaxation process.

Finally, it may be concluded that the flare phenomena in AR 5747 can be accounted for by the " storage followed by release" model, where the energy is stored more or less continuously, but it is released suddenly and catastrophically (Rust et al. 1994).

We wish to thank Dr. Metcalf for allowing us to use some of his numerical routines for analyzing vector magnetograms. We also thank Dr. J. W. Lee and Dr. Pevtsov for helpful comments. The data from the Mees Solar Observatory, University of Hawaii are produced with the support of NASA grant NAG 5-4941 and NASA contract NAS8-40801. This work has been supported in part by Basic Research Fund of Korea Astronomy Observatory, by BSRI Program (BSRI-98-5408), and by BK21 Project, Ministry of Education. GSC was supported by the DoE Contract No. DE-AC02-76-CHO3073 and the NSF grant ATM-9906142.

REFERENCES

Canfield, R. C., La Beaujardiere, J.-F., Han, Y., Leka, K. D., McClymont, A. N., Metcalf, T. R., Mickey, D. L., Wulser, J.-P., & Lites, B. W. 1993, ApJ, 411, 362

Demoulin, P., van Driel-Gesztelyi, L., Schmeider, B., Hénoux, J. C., Gsepura, G., & Hagyard, M. J. 1993, A&A, 271, 292

Demoulin, P., Hénoux, J. C., Priest, E. R., & Mandrini, C. H. 1996, A&A, 308, 643

Hagyard, M.J., Low, B.C., & Tandberg-Hanssen, E. 1981, Sol. Phys., 73, 257

Hagyard, M. J., Smith, Jr., J. B., Teuber, D., & West, E. A. 1984, Sol. Phys., 91, 115

Hagyard, M. J., Ventkatarishnan, P., & Smith, Jr., J. B. 1990, ApJS, 73, 159

Leka, K. D., Canfield, R. C., McClymont, A. N., de la Beaujardiere, J. F., & Fan, Y. 1993, ApJ, 411, 370

Lü, Y., Wang, J., & Wang, H. 1993, Sol. Phys., 148, 119

McClymont, A. N., Jiao, L., & Mikić, Z. 1997, Sol. Phys., 174, 191.

Metcalf, T. R., Jiao, L., McClymont, A. N., Canfield, R. C., & Uitenbroek, H. 1995, ApJ, 439, 474

Mickey, D. L. 1985, Sol. Phys., 97, 223

Moon, Y.-J., Yun, H. S., & Park, Y.D. 1996a, JKAS, S323

Moon, Y.-J. 1999, Ph. D. Thesis, Seoul National University

Moon, Y.-J., Yun, H. S., Lee, S. W., Kim, J.-H. Choe, G. S., Park, Y. D., Ai, G., Zhang, H., & Fang, C. 1999, Sol. Phys., 184, 323

Moon, Y.-J., Yun, H. S., Choe, G. S., Park, Y. D., & Mickey, D. L. 2000, submitted to Solar Physics

Pevtsov, A.A., Richard, C.C., & McClymont, A. N. 1997, ApJ, 481, 973

Ronan, R. S., Mickey, D. L., & Orral, F. Q. 1987, Sol. Phys., 113, 353

Rust, D. M., Sakurai, T., Gaizauskas, V., Hofmann, A., Martin, S. M., Priest, E. R., & Wang, J. 1994, Sol. Phys., 153, 1

Skumanich, A., & Lites, B. W. 1987, ApJ, 322, 473

Wang, H. 1992, Sol. Phys., 1992, 140, 85

Wang, H. 1997, Sol. Phys., 174, 163

Wang, J., Shi, Z., Wang, H., & Lue, Y. 1996, ApJ, 456, 861

Wang, T., Xu, A., & Zhang, H. 1994, Sol. Phys., 155. 99